Faraday Discussions

Accepted Manuscript

This manuscript will be presented and discussed at a forthcoming Faraday Discussion meeting. All delegates can contribute to the discussion which will be included in the final volume.

Register now to attend! Full details of all upcoming meetings: **http://rsc.li/fd-upcoming-meetings**

This is an *Accepted Manuscript*, which has been through the RSC Publishing peer review process and has been accepted for publication.

Accepted Manuscripts are published online shortly after acceptance, which is prior to technical editing, formatting and proof reading. This free service from RSC Publishing allows authors to make their results available to the community, in citable form, before publication of the edited article. This *Accepted Manuscript* will be replaced by the edited and formatted *Advance Article* as soon as this is available.

To cite this manuscript please use its permanent Digital Object Identifier (DOI®), which is identical for all formats of publication.

More information about *Accepted Manuscripts* can be found in the **Information for Authors**.

Please note that technical editing may introduce minor changes to the text and/or graphics contained in the manuscript submitted by the author(s) which may alter content, and that the standard **Terms & Conditions** and the **ethical guidelines** that apply to the journal are still applicable. In no event shall the RSC be held responsible for any errors or omissions in these *Accepted Manuscript* manuscripts or any consequences arising from the use of any information contained in them.

CREATED USING THE RSC LaTeX PCCP ARTICLE TEMPLATE – SEE www.rsc.org/electronicfiles FOR DETAILS
PAPER www. rsc.org/faraday_d | Faraday Discussions

Application of a diffusion-desorption rate equation model in astrochemistry

Jiao He[a] **and Gianfranco Vidali***[a]

Received Xth XXXXXXXXXX 20XX, Accepted Xth XXXXXXXXX 20XX
First published on the web Xth XXXXXXXXXX 200X
DOI: 10.1039/c000000x

Desorption and diffusion are two of the most important processes on interstellar grain surfaces; knowledge of them is critical for the understanding of chemical reaction networks in interstellar medium (ISM). However, lack of information on desorption and diffusion is preventing further progress in astrochemistry. To obtain desorption energy distributions of molecules from surfaces of ISM-related materials, one usually carries out adsorption-desorption temperature programmed desorption (TPD) experiments, and use rate equation models to extract desorption energy distributions. However, the often-used rate equation models fail to adequately take into account diffusion processes and thus are only valid in situations where adsorption is strongly localized. As adsorption-desorption experiments show that adsorbate molecules tend to occupy deep adsorption sites before occupying shallow ones, a diffusion process must be involved. Thus, it is necessary to include a diffusion term in the model that takes into account the morphology of the surface as obtained from analyses of TPD experiments. We take the experimental data of CO desorption from the MgO(100) surface and of D_2 desorption from amorphous solid water ice as examples to show how a diffusion-desorption rate equation model explains the redistribution of adsorbate molecules among different adsorption sites. We extract from TPD profiles distributions of desorption energies and diffusion energy barriers. These examples are contrasted with a system where adsorption is strongly localizes - HD from an amorphous silicate surface. Suggestions for experimental investigations are provided.

1 Introduction

The kinetics of interstellar related species on dust grain surfaces are known to play an important role in astrochemistry. Astrochemical modeling shows that the abundances of molecules such as H_2, H_2O and CO_2 can't be explained by gas-phase reactions alone, and surface reactions must be involved.[1–3] Desorption and diffusion are the two most important processes on surfaces, and these determine the rates of surface reactions. In recent years there has been a considerable body of work on the surface kinetics of ISM (interstellar medium) - related species. Katz et al.[4] used rate equations to extract desorption and diffusion energy barriers for atomic hydrogen from the data on formation of molecular hydrogen

[a] *Syracuse University, 201 Physics Bldg., Syracuse, NY 13244-1130 (USA). E-mail: gvidali@syr.edu*

of Pirronello et al.[5,6] on polycrystalline olivine and amorphous carbon surfaces. Cazaux and Tielens[7] came up with a similar model that included the possibility of diffusion by tunneling and the possibility of the atom dropping in a chemisorption site. Iqbal et al.[8] studied the formation of molecular hydrogen over a wider range of surface temperature using a kinetic Monte Carlo simulation in order to simulate the formation of molecular hydrogen in regions, such as PDRs (photodissociation regions) where grains are at a temperature higher than in diffuse and dense clouds. Amiaud et al.[9,10] conducted D_2 adsorption-desorption experiments on both porous and non-porous amorphous water ices, and used a rate equation model and a direct inversion method to obtain desorption energy barriers. Noble et al.[11] did experiments of desorption of CO, O_2 and CO_2 from non-porous water ice, crystalline water ice and silicate surfaces, and used a Polanyi-Wigner equation to find the parameters governing desorption behaviors. He et al.[12] used multiple desorption energy levels to simulate adsorption-desorption experiments of D_2 on both single crystalline and amorphous silicate surfaces, and obtained semi-continuous desorption energy distributions. Desorption energies for a variety of ices, including ice mixtures, are summarized by Burke and Brown.[13] All of these investigations assumed either non-hopping between different desorption sites or adlayer equilibration.[14] Thus only the desorption energy can be obtained.

Diffusion of radicals is an obvious important step in the formation of molecules in or on ices. Because of its abundance and low mass, diffusion of H atoms is the most important process. H diffusion in CO ice leads to the formation of H_2CO and CH_3OH.[15–18] H diffusion in N_2 leads to ammonia formation[19] and H diffusion in O_2 ices leads to the formation of water.[20,21] In general, the formation of molecules on surfaces require diffusion to take place, such as in the case of the formation of water via the deposition of H, O and O_2 on water ice[22,23] and on bare amorphous silicates.[24,25] Similarly, the formation of molecules due to energetic particles or radiation involves the migration of super thermal radicals.[26] Except in the investigation of the formation of D_2 by the bombardment of CD_4 ice with 5 keV electrons where rate equations were used to obtain the diffusion energy barrier for deuterium atoms,[27] the analyses of these and other reactions don't contain estimates of diffusion energy barriers or diffusion coefficients.

The diffusion of larger molecules can also take place in or on ices and on bare surfaces. Mispelaer et al.[28] studied the diffusion of CO, HNCO, H_2CO and NH_3 in amorphous ice using infrared spectroscopy, while He et al. investigated the formation of ozone via the diffusion of molecular and atomic oxygen on a bare amorphous silicate surface.[29] Zubkov et al.[30] studied the diffusion of nitrogen in amorphous solid water, and Roser et al. studied the formation of CO_2 via the migration of O in a water-ice capped CO ice.[31] Because diffusion is more difficult to study than desorption, both experimentally and theoretically, much less information about diffusion on interstellar grain surfaces is available than that of desorption. It is often assumed that the energy barrier for thermal diffusion $E_{\rm diff}$ is a fraction of the desorption energy $E_{\rm des}$, $E_{\rm diff} = \alpha E_{\rm des}$, where α is taken to be a constant value typically between around 0.3 for weakly adsorbed systems on well ordered surfaces.[32] However, results of simulations of data of molecular hydrogen formation on disordered or amorphous surfaces of silicates and water ice yield a larger value of α (0.7-0.8).[4,33,34] Since these simulations can give only a lower bound for the hydrogen desorption energy (E_{des}), the value of α could

be lower. Simulations of ISM chemistry that include surface reactions have used such a wide range of values as well.[8,35,36]

In any case, this relation $E_{\rm diff} = \alpha E_{\rm des}$ is an oversimplification. Since the diffusion energy barrier is in the exponential term of Polanyi-Wigner equation, a slight change in α could affect the diffusion rate by orders of magnitude, resulting in unrealistic reaction rates. Surface diffusion occurs both by quantum tunneling and by thermally activated hopping. Quantum tunneling is efficient for very light adsorbed species such as atomic[17] and molecular hydrogen,[37] but the efficiency decreases dramatically as the ad-species mass increases. Furthermore, quantum tunneling depends on both the energy barrier and the separation to the site the particle is tunneling into. It typically decreases dramatically for disordered or amorphous surfaces. Hama et al.[38] studied the diffusion of hydrogen atoms on the surface of amorphous ice, using a combination of photon-stimulated desorption and REMPI (Resonance Enhanced MultiPhoton Ionization) and found that hydrogen becomes trapped at deep sites, confirming the indirect evidence obtained in the study of H_2 formation on silicates and amorphous carbon[4,6,39] and on amorphous silicates.[34] For ad-species other than hydrogen, thermal diffusion is the dominant diffusion mechanism, and this will be the focus of this paper.

The remaining of this paper is organized as follows. In the next section we summarize the most general form of a rate equation model and discuss its limitations, then in Section 3 we present the diffusion-desorption rate equation model, and in Section 4 we apply it to the systems CO on MgO(100),[40] D_2 on non-porous water ice,[10] and HD on amorphous silicate surface, followed by a discussion of the limitations and suggestions for experimental investigations. In Section 5 we summarize the paper.

2 Rate equation model

Temperature programmed desorption (TPD)[41,42] has been used widely as a tool to study gas-surface interactions in astrochemistry, such as adsorption-desorption and surface diffusion.[9,10,12,13,40,43–45] A typical TPD experiment consists of two stages, the exposure stage in which the substrate surface is exposed to adsorbate particles, and the warm-up stage in which the substrate surface is warmed up to desorb adsorbate material. A mass spectrometer is placed in the vacuum chamber to monitor desorbing particles from the surface. Interpretation of TPD spectra is generally carried out using the Polanyi-Wigner rate equation; assuming first order desorption, the desorption rate can be written as:

$$R(t) \propto -\frac{d\theta(t)}{dt} = \nu\theta(t)\exp\left(-\frac{E_{\rm des}}{k_{\rm B}T(t)}\right) \quad (1)$$

where $R(t)$ is the desorption rate, ν is the desorption pre-exponential factor that depends on the substrate and adsorbate - hereafter we use the standard value of $10^{12}/sec.$, $\theta(t)$ is the coverage defined as percentage of 1 ML, i.e., the number of adsorbate particles divided by the number of adsorption sites on the surface, $E_{\rm des}$ is the desorption energy, $k_{\rm B}$ is Boltzmann constant, $T(t)$ is the temperature of the surface. This is a simple model assuming all surface sites are identical. In reality, however, a surface consists of different adsorption sites, and to better describe

the desorption behavior a continuous desorption energy distribution $f(E_{\rm des})$ is required. We modify the rate equation as:

$$\int f(E_{\rm des})\, dE_{\rm des} = 1 \tag{2}$$

$$\frac{d\theta(E_{\rm des},t)}{dt} = flux(t)(1-\theta(E_{\rm des},t)) - \nu\theta(E_{\rm des},t)\exp\left(-\frac{E_{\rm des}}{k_{\rm B}T(t)}\right) \tag{3}$$

$$R(t) = \int\left(flux(t)\theta(E_{\rm des},t) + \nu\theta(E_{\rm des},t)\exp\left(-\frac{E_{\rm des}}{k_{\rm B}T(t)}\right)\right) f(E_{\rm des})\, dE_{\rm des} \tag{4}$$

Eq.(2) gives the desorption energy distribution, Eq.(3) gives the coverage as a function of time for different sites, the $(1-\theta(E_{\rm des},t))$ is the rejection term to avoid multiple occupancy of the same site, Eq.(4) describes the desorption rate plus reflection of the incoming flux, which is proportional to the measured mass spectra signal. The integration in Eq.(2) and Eq.(4) are over the whole desorption energy spectrum.

This set of equations forms the basis for interpretation of most adsorption-desorption experiments. The more energy levels used in the modeling, the smoother the energy distribution becomes. In He et al[12] more than 50 energy levels were used to fit the TPD spectra; a semi-continuous desorption energy distribution was obtained for both amorphous and single crystalline silicates. To obtain a continuous desorption energy distribution, some groups used a direct inversion method based on first order desorption to extract information from TPD spectra;[46] a more detailed analysis can be found in Barrie et al.[47] All these analyses are based on first order desorption without diffusion. We show below that diffusion is necessary to explain the experimental data.

In some systems, however, it is found that the desorption energy is coverage dependent; as coverage increases from 0 to 1 ML, the TPD peak shifts to lower temperatures, as shown in Dohnálek et al[40] and Amiaud et al[10] (referred to as Dohnálek2001 and Amiaud2007 hereafter). There are two different explanations for the temperature shift, one is adsorbate lateral interactions, the other is hopping between different adsorption sites. For the former, lattice-gas modeling has been used to simulate the effect of lateral integration on TPD shapes,[14,48,49] and fitting with TPD traces can be obtained. However, in the interstellar medium the coverage of ad-species on grain surfaces is typically very small (much smaller than 1 ML). In low coverage experiments that find applications in astrochemistry, the morphology and hopping between different adsorption sites of the surface contribute more to the desorption than lateral interactions. Therefore, in this paper we focus on the effects of hopping and ignore lateral interactions. In the exposure stage, particles tend to occupy deeper adsorption sites before they occupy the shallower sites. The intrinsic physical process underlying this phenomenom is surface diffusion, i.e., when adsorbate particles are in the shallow sites, the diffusion energy barrier is also low. Particles escape from the shallow adsorption site and move on the surface until they reach deeper sites where the diffusion energy barrier is high enough that they are trapped.

In analysis of CO desorption from MgO TPD experimental data, Dohnálek2001 used an inversion method to extract a continuous coverage dependent desorption energy distribution, and the extracted spectrum can reproduce experimental traces very well. It should be noted that the direct inversion method is only applicable to equilibrium diffusion state, in which the mobility of particles on a surface is so fast that particles are already in an equilibrium state before desorption begins. By using the direct inversion method Dohnálek2001 and Amiaud2007 implicitly assume that the mobility of adsorbate particles is fast enough, i.e., diffusion rate is high enough that the adsorbate is equilibrated. The effect of limited mobility of ad-species was discussed by Surda et al[50] but, to best of our knowledge, this work has not been used in astrochemistry. In the next section we introduce the diffusion-desorption rate equation that was inspired by the work of Surda et al.[50]

3 The diffusion-desorption rate equation model

An adsorption-desorption experiment involves both desorption and diffusion processes. Hereby, the desorption rate and diffusion rate both depend on the substrate surface temperature,. Below, we assume that both obey an Arrhenius-like expression. The desorption rate for sites with desorption energy $E_{\rm des}$ can be expressed as $\nu\theta(E_{\rm des},t)\exp\left(-\frac{E_{\rm des}}{k_{\rm B}T(t)}\right)$; similarly the diffusion rate is $\nu_{\rm diff}\theta(E_{\rm des},t)\exp\left(-\frac{E_{\rm diff}}{k_{\rm B}T(t)}\right)$, where $E_{\rm diff}$ is the diffusion energy barrier for those sites with desorption energy $E_{\rm des}$. There is a direct positive relation between $E_{\rm des}$ and $E_{\rm diff}$, i.e., sites with higher desorption energy also have higher diffusion energy barriers. Distinction is made between the two pre-factors $\nu_{\rm diff}$ and ν, since they corresponds to different physical processes and could have different values. Diffusion consists of two subprocesses: 1) particles hop out of adsorption sites and go to a transition state; 2) particles in the transition state go back to the adsorption sites. There is a redistribution in the second subprocess depending on the availability of adsorption sites. If a particle can go on top of another in the same adsorption site, particles in transition states will be redistributed evenly among all adsorption sites. The redistribution obeys the same distribution as the desorption energy; otherwise, if a particle cannot go on top of another, the particle in the transition state will be redistributed evenly among all *empty* sites; hereafter we assume the latter case.

The desorption energy is a continuous distribution. Let us assume it can be represented by a single Gaussian distribution. As is shown in Fig. 1, the diffusion energy barrier $E_{\rm diff}$ is the difference between the desorption energy $E_{\rm des}$ and the energy at the transition state $E_{\rm tr}$, $E_{\rm diff}=E_{\rm des}-E_{\rm tr}$. Suppose that $E_{\rm tr}$ follows also a Gaussian distribution, then we express these two distributions as

$$f(E_{\rm des})=\frac{1}{\sigma_{des}\sqrt{2\pi}}\exp\left(-\frac{(E_{\rm des}-\overline{E_{\rm des}})^2}{2\sigma_{des}^2}\right)$$

$$f(E_{\rm tr})=\frac{1}{\sigma_{tr}\sqrt{2\pi}}\exp\left(-\frac{(E_{\rm tr}-\overline{E_{\rm tr}})^2}{2\sigma_{tr}^2}\right)$$

Assuming that these two distributions are independent, then $E_{\rm diff}$ is also a Gaussian distribution, with $\overline{E_{\rm diff}}=\overline{E_{\rm des}}-\overline{E_{\rm tr}}$ and $\sigma_{diff}=\sqrt{\sigma_{des}^2+\sigma_{tr}^2}$.

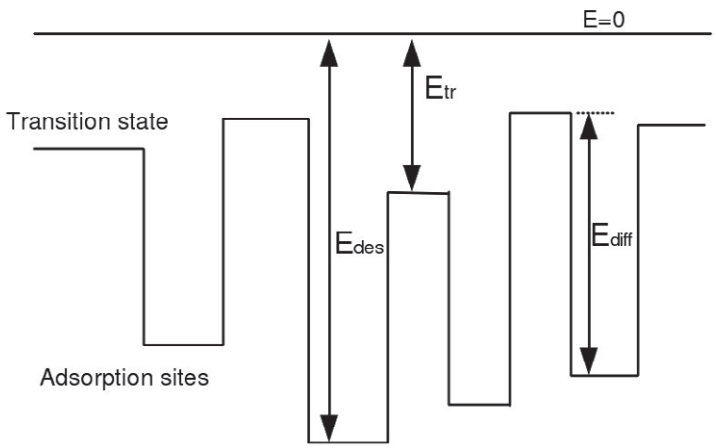

Fig. 1 Diagram of surface adsorption sites and transition states.

If we further assume that $\overline{E_{\rm diff}}$ is not far from $\overline{E_{\rm des}}$ - it has been suggested $E_{\rm diff} \sim 0.5\text{-}0.7 E_{\rm des}$,[4,34,51] then $\sigma_{\rm tr}^2$ should be much smaller than $\sigma_{\rm des}^2$, we assume $\sigma_{\rm diff} = \sqrt{\sigma_{\rm des}^2 + \sigma_{\rm tr}^2} \approx \sigma_{\rm des}$, which means that $E_{\rm diff}$ can be approximated by $E_{\rm diff} = E_{\rm des} - \overline{E_{\rm tr}} = E_{\rm des} - \Delta E$. If $E_{\rm tr}$ and $E_{\rm des}$ are dependent, perhaps the approximation $E_{\rm diff} = \alpha E_{\rm des}$ [52] is appropriate. A more general expression would be $E_{\rm diff} = \alpha(E_{\rm des} - \Delta E)$.

Now Eq.(3) should be modified as follows:

$$\begin{aligned}
&\frac{d\theta(E_{\rm des},t)}{dt} \\
&= \underbrace{flux(t)(1-\theta(E_{\rm des},t))}_{term\ 1} - \underbrace{\nu\theta(E_{\rm des},t)\exp\left(-\frac{E_{\rm des}}{k_{\rm B}T(t)}\right)}_{term\ 2} \\
&\quad \underbrace{-\nu_{\rm diff}\theta(E_{\rm des},t)\exp\left(-\frac{\alpha(E_{\rm des}-\Delta E)}{k_{\rm B}T(t)}\right)}_{term\ 3} \\
&\quad \underbrace{+\frac{1-\theta(E_{\rm des},t)}{1-\Theta(t)}\int\nu_{\rm diff}\theta(E'_{\rm des},t)\exp\left(-\frac{\alpha(E'_{\rm des}-\Delta E)}{k_{\rm B}T(t)}\right)f(E'_{\rm des})dE'_{\rm des}}_{term\ 4}
\end{aligned} \tag{5}$$

$$\Theta(t) = \int\theta(E_{\rm des},t)f(E_{\rm des})dE_{\rm des} \tag{6}$$

Eq.(2) and Eq.(4) are unchanged. In Eq.(5) term 1 is the flux term, assuming particles cannot go on top of each other; term 2 is the desorption term; term 3 is the diffusion term that describes particles that go to transition states; term 4 is the redistribution term from the transition states, assuming particles can only go to

empty sites; the factor $(1-\theta(E_{\rm des},t))/(1-\Theta(t))$ accounts for the redistribution of particles in transition states among empty adsorption sites. In Eq.(6) $\Theta(t)$ is the overall coverage. Note that integration of terms 3 and 4 over the whole energy spectrum gives zero; this means that in diffusion processes the total particle number is conserved, which should hold true for the model to be correct since diffusion alone won't change the total number of particles on the surface. The diffusion term is no longer a first order term. In fact it behaves like a second order term. Thus the modified rate equation model is a candidate to interpret coverage dependent desorptions. A comparison with the complete model in Li et al[53] (referred to as Li2010 hereafter) is worth mentioning here. It can be shown that in the low coverage limit, this model is equivalent to Eq.(5) in Li2010; however, at coverage approaches 1 ML they differ. In Li2010 it is assumed that at a coverage close to 1 ML the diffusion rate is close to 0; however in this paper we assume the probability that particles jump out from adsorption sites to transition sites is independent of coverage, which leads to the exchange of particles among adsorption sites and a faster redistribution. The calculated diffusion rate is thus faster in this work than in Li2010.

4 Simulations and discussion

4.1 CO on MgO(100)

Below we illustrate how to utilize the rate equation model to extract the adsorption-diffusion energy parameters. The experimental data are taken from Dohnálek2001, where a detailed description of the experiment can be found. A highly ordered MgO(100) surface kept at 22 K was exposed to different doses of CO gas in ultra-high vacuum. The MgO(100) film was grown epitaxially on an Mo(100) substrate at 600 K by evaporation of Mg metal in an O_2 atmosphere. The dose of CO was calculated by integration of TPD traces to be θ=(0.09, 0.16, 0.23, 0.32, 0.42, 0.48, 0.58, 0.71, 0.90, 1.00, 1.14, 1.27) ML. Below we only discuss the submonolayer range, omitting the last two coverages. After exposure the thin film surface was subjected to a linear heating ramp of $\beta = dT/dt = 0.6K/sec$ to desorb the CO molecules. The TPD traces are shown in Fig. 2. We begin with the direct inversion of Eq.(1); the coverage dependent desorption energy can be calculated for each TPD trace as follows:

$$E(\theta) = -k_{\rm B}T\ln\left(-\frac{\beta}{\nu\theta}\frac{d\theta}{dT}\right) \tag{7}$$

The resulting desorption energy distribution $f(E_{\rm des})$ is shown in Fig. 3.

In Dohnálek2001, TPD traces for different initial coverages are inverted and different pre-exponential factors are tried until convergence is achieved among the inverted distributions from different initial coverages. They found $\nu = 10^{15}/sec$.. In our opinion this value should be revised. Nordholm et al.[54] found that abnormally large pre-exponential factors might come from dispersion in the desorption energy. Thus, to determine the pre-exponential factor using convergence might be incorrect. ν is a fundamental factor that depends on both the substrate and the adsorbate, and its value is better to be determined by ab-initio calculations.

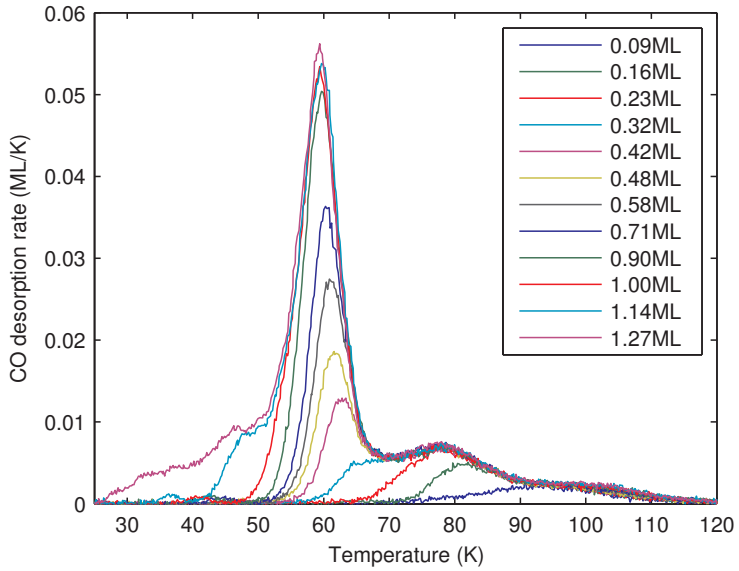

Fig. 2 CO TPD spectra for monolayer and submonolayer coverages of CO/MgO(100) (θ = 0.09, 0.16, 0.23, 0.32, 0.42, 0.48, 0.58, 0.71, 0.90, 1.00, 1.14, 1.27). Replotted from Dohnálek2001.[40]

We are not aware of such calculations for the present system. Therefore, we prefer to use the widely accepted value $\nu = 10^{12}/sec.$. For $\nu_{\rm diff}$ there is even less information available, and we use the same value as ν for simplicity. To do the inversion, we pick the trace with the highest submonolayer coverage from TPD data.

In Eq.(5) if one lets $\nu_{\rm diff} = 0$ then the diffusion-desorption rate equation is a rate equation for non-hopping ad-species. The simulated TPD traces are shown in Fig. 4. Next we set ν and the flux equal to 0 , i.e., we assume no incoming flux and no desorption, and we focus on the diffusion process. We start from an initial coverage of 0.3 ML for all desorption sites with $\Delta E = 30$ meV, $\nu_{\rm diff} = 10^{12}/sec.$, and then monitor the redistribution process during warm-up. Fig. 5 shows the fractional occupation distribution at temperature 22 K, 40 K, 45 K, 50 K, 55 K, 60 K, 65 K, 70 K and 75 K. As is shown in the figure, at 22 K and 40 K, the surface has a uniform coverage of 0.3 ML. When the surface temperature rises to 45 K, molecules in shallow sites ($E_{\rm des} < 150$ meV) become active and begin to diffuse, distributing themselves evenly among deeper sites which have not been occupied yet. As temperature rises further, deeper sites come into play and molecules begin to diffuse. After the temperature reaches a point where the deepest sites are occupied (about 65 K in this case), the distribution doesn't change any more as we increase the temperature further. This means that when the diffusion rate is high enough, the coverage distribution doesn't change as the diffusion rate is further increased. In the fast diffusion case one cannot get the absolute value of the diffusion energy barrier, only a lower bound is obtainable, or equivalently, a lower bound for ΔE. What one sees in TPD is that molecules

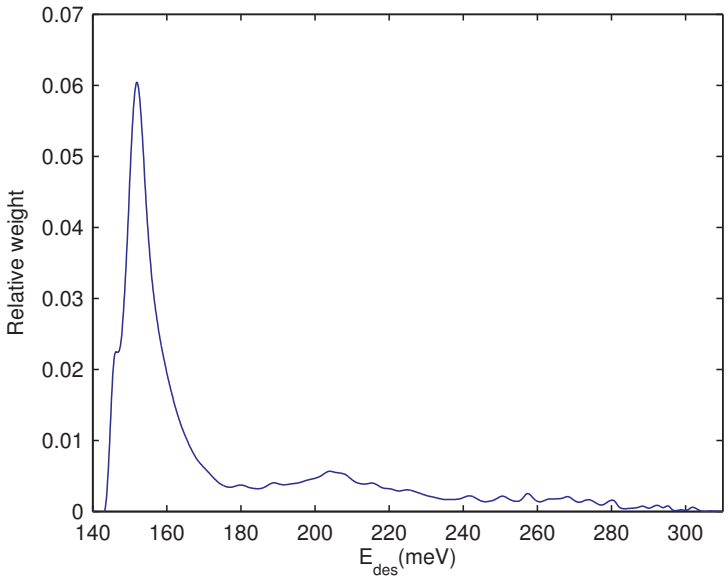

Fig. 3 Desorption energy barrier distribution for CO on MgO(100) obtained using data of Dohnálek2001[40]

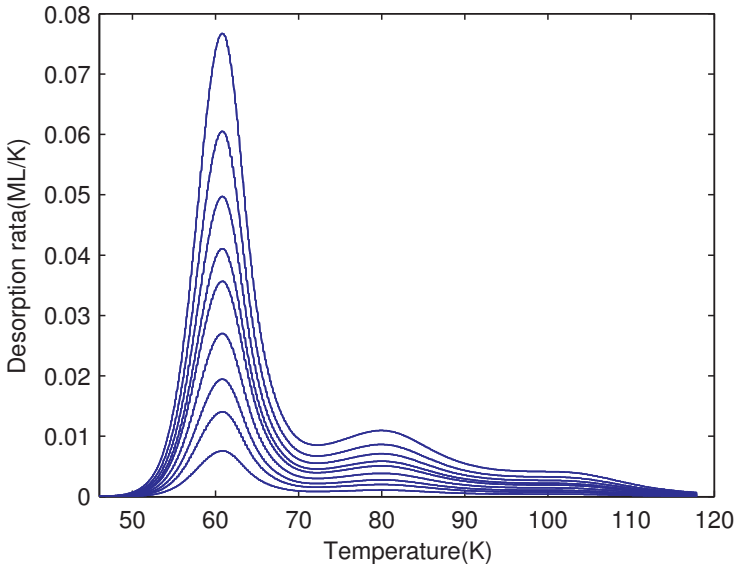

Fig. 4 Simulation of TPD spectra for different initial coverages using the desorption energy distribution obtained from direct inversion of CO on MgO(100) TPD spectra of Dohnálek2001,[40] see Fig. 3.

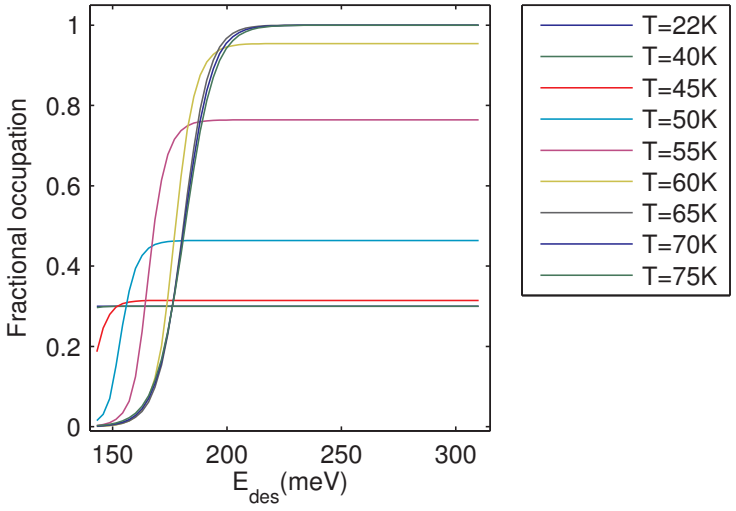

Fig. 5 Fractional occupation of adsorption sites at different temperatures: 22 K, 40 K, 45 K, 50 K, 55 K, 60 K, 65 K, 70 K and 75 K. No desorption is assumed and only the diffusion process is simulated. The initial coverage and ΔE are 0.3 ML and 30 meV, respectively. As the temperature increases, molecules move from shallow adsorption sites to deeper ones.

occupy deeper sites before they go to shallower sites, and the TPD trailing edges for different initial coverages should converge. This justifies the use of the direct inversion method, since the direct inversion method assumes that molecules automatically occupy the deepest sites available on the surface . On the other hand, if the diffusion rate is limited, ad-species start to desorb and leave the surface before an equilibrium state is achieved.[50] If one plots the weighted overall desorption rate and diffusion rate as a function of temperature, the two traces might overlap each other. If the overlapping is small, i.e., the desorption starts after most molecules have begun to diffuse, the assumption of fast diffusion holds true. However, if the two traces overlap significantly, an equilibrium state cannot be obtained before desorption begins, and the direct inversion method is less applicable. In this latter case, the diffusion-desorption rate equation model should be used.

Now we show how to obtain the $E_{\rm diff}$ distribution or equivalently, the value (or range) of ΔE. We try different values of ΔE in Eq.(5) and simulate TPD for different initial values of the coverage until we find the value that best fit experimental data. The results are shown in Fig. 6. It can be seen from the simulation results that when ΔE is small the TPD traces are similar to first order desorption with high localization. As ΔE increases the gaps between trailing edges decrease. When ΔE is greater than 30 meV there are almost no gaps, and the shape of TPD traces doesn't change as the ΔE value is increased further. Thus we only get a lower boundary for ΔE in the case of fast diffusion. This is consistent with our previous argument.

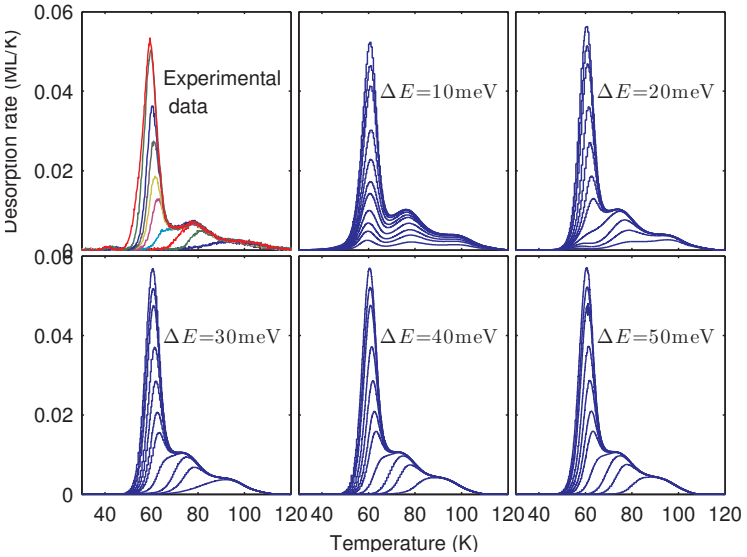

Fig. 6 Simulation of Dohnálek2001[40] experimental data using different ΔE values, based on the diffusion-desorption rate equation model. The experimental data are shown in the first panel.

4.2 D_2 on amorphous water ice

H_2/D_2 plays an important role in interstellar chemistry. Here we examine D_2 adsorption-desorption on non-porous amorphous water ice as a second example of how to obtain desorption and diffusion energy barriers. The experiments are reported in Amiaud et al.[10] The water ice films were grown on a copper surface using a microchannel array doser. The morphology was checked to be non-porous amorphous by N_2 adsorption/desorption TPD experiments. The sample was kept at 10 K and exposed to various doses of D_2. After exposure, a TPD was carried out with a heating rate of 10 K/min. The TPD spectra are shown in Fig. 7. Following the same direct inversion procedure as discussed above, we obtain a desorption energy barrier distribution $E_{\rm des}$ as shown in Fig. 8. From the so-obtained $E_{\rm des}$ distribution, we simulate TPD spectra for different ΔE values. The results are shown in Fig. 9. Next, we compare the simulation results and the experimental TPD profiles to find out the best ΔE value. Notice that in the trailing edge of the TPD profiles there are gaps between traces. As is clear from previous discussion and Fig. 6, if the diffusion rate is fast enough there shouldn't be gaps in the trailing edges; thus, the diffusion rate is not fast enough, and this looks like desorption of non-equilibrated film. A best fit gives $\Delta E = 2$ meV. If the gaps in the trailing edge are due to the limited pumping speed in the vacuum chamber, the experimental TPD traces should be corrected for it. This may reduce the gaps in trailing edges and make the experimental TPD peaks sharper. If after pumping speed corrections there are no gaps at all, then the best fit is with $\Delta E \geq 6$ meV. In this case we would have a lower limit of ΔE. The pumping speed corrections are not presently available for this system.

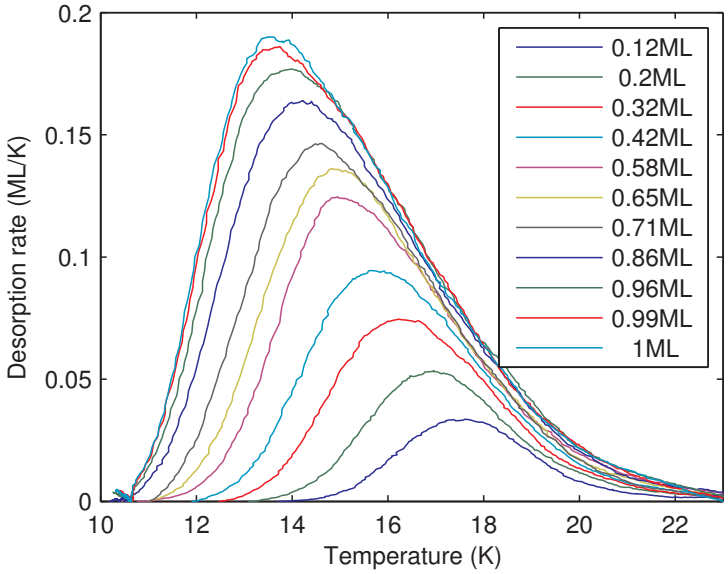

Fig. 7 TPD spectra for D_2 adsorption-desorption from np-amorphous water ice; the surface temperature during exposure with D_2 is 10 K. Data from Amiaud et al.[10]

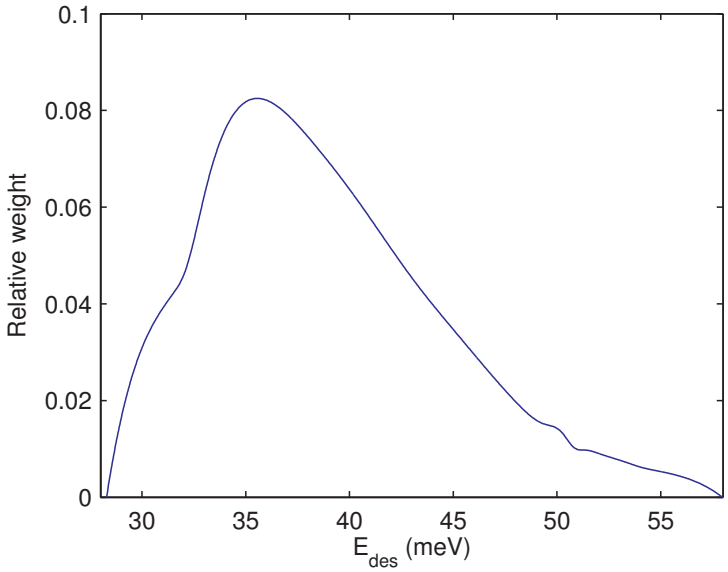

Fig. 8 Desorption energy barrier distribution for D_2 obtained from the model using np-amorphous water ice data of Amiaud et al.[10]

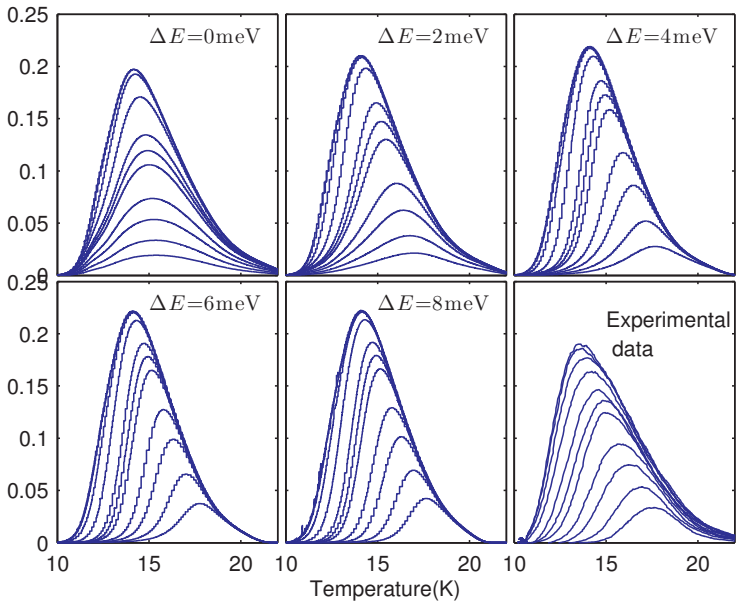

Fig. 9 Simulation of adsorption-desorption TPD spectra of Amiaud et al.[10] using different ΔE values; the original experimental data are also shown for comparison.

4.3 HD on an amorphous silicate

Here we analyze the HD desorption from an amorphous silicate surface. The sample was prepared by Dr. Brucato (then at the Osservatorio Astronomico di Capodimonte Naples) by laser ablation of targets in an oxygen atmosphere. The experimental set-up and measuring methods are similar as the ones described in Perets et al.[34] To summarize: an amorphous silicate ($FeMgSiO_4$) sample was kept at 10.5 K and exposed to an HD beam flux for 30 sec, 1 min, 2 min, 4 min and 8 min. Coverage calibration is unavailable, but it's known that the coverages are well below 1 ML. After exposure the surface was warmed up by cutting off the liquid helium flow. A reproducible heating curve is achieved for different TPD runs. The TPD traces are shown in Fig. 10. Applying the direct inversion method to the trace of 4 min exposure, which is a typical one, we obtain the desorption energy distribution shown in Fig. 11. The TPD spectra are typical to first order desorption without hopping; this indicates that the diffusion energy barriers are similar or even higher than the desorption energies so that diffusion doesn't take place before desorption.

4.4 Limitations and suggestions for experimental investigations

As we have seen in the first two examples, although we are able to obtain good fits for the adsorption-desorption TPD profiles, we can get only a lower limit to ΔE. Furthermore, we considered only thermally activated diffusion since this is what several experiments suggest. Based on our analyses, we suggest steps in future investigations that could facilitate the extraction of important parameters. In

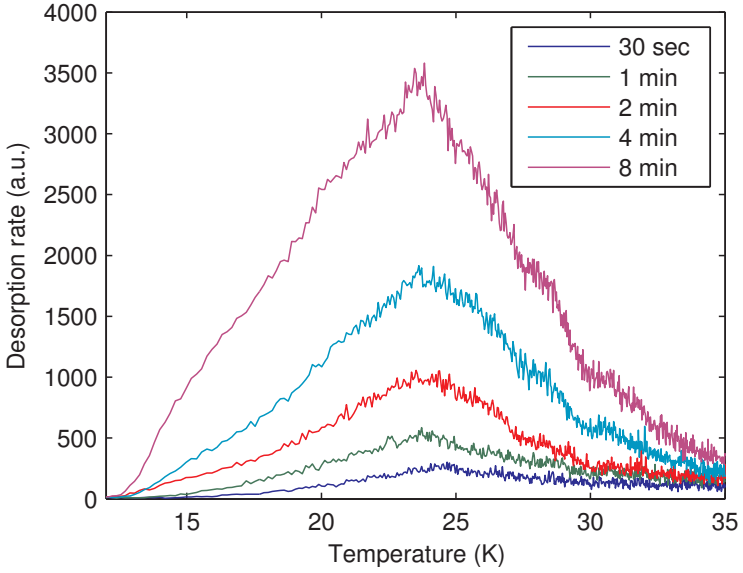

Fig. 10 HD desorption from amorphous silicate ($FeMgSiO_4$) surface. The exposure doses are 30 sec, 1 min, 2 min, 4 min and 8 min. The surface temperature during exposure with HD is 10.5 K.

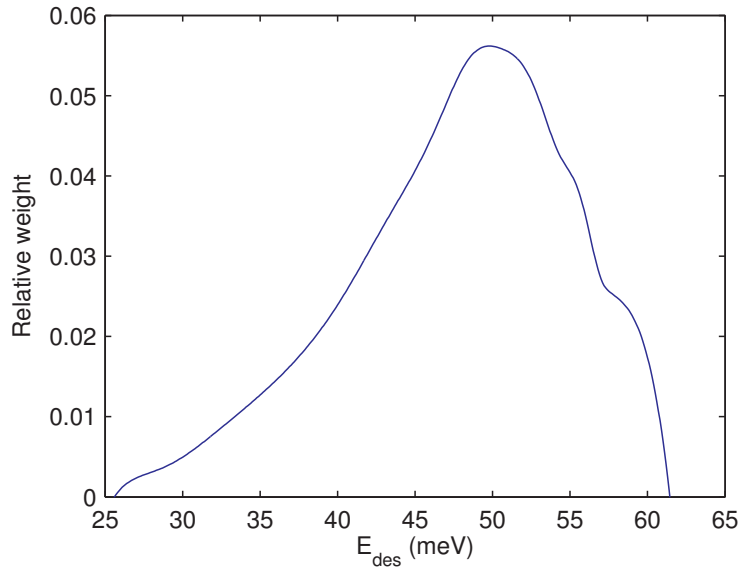

Fig. 11 HD desorption energy distribution obtained from direct inversion of the TPD spectra in Fig. 10.

experimental investigations, efforts should be made to push the film in a far from equilibrium state to separate the trailing edges. This is done with flash desorption in many surface science studies[42] but it poses technical challenges for surfaces kept at liquid helium temperature. It would be advantageous to study films at very low coverages, since the differences in TPD traces with different ΔE are most significant when coverages is low, as can be seen in Fig. 6. Furthermore, special care needs to be paid to the pumping speed, background noise and desorption from parts other than the sample, since these affect the TPD traces, especially the tailing edges.

5 Conclusions

In this paper we discussed the limitation of the often-used rate equation model when simulating adsorption-desorption TPD experimental profiles, and introduced a diffusion-desorption rate equation model to take into account the diffusion processes. Desorption and diffusion energy barrier distributions are obtained for CO on MgO(100) and D_2 on np-amorphous water ice. We then presented a system, HD desorption from an amorphous silicate, where there is hardly any evidence of diffusion. These distributions, or information obtained from them, can be used in models of the chemical evolution of interstellar medium environments. For example, Herbst et al.[55] and Iqbal et al.[8] have taken into consideration in their kinetic Monte Carlo models the morphology of the surface in the formation of molecular hydrogen on surfaces. At that time, little or no information was available on diffusion energy barriers and on distribution of adsorption of energy sites besides a little more than rules of thumb. Now we have shown that using existing TPD data it is possible to tease out important information on the energetics of adsorption/desorption and diffusion. Furthermore we have made suggestions for future experimental investigations so analyses of those data will yield more detailed information on these important processes that are at the heart of molecule formation on interstellar dust grains.

Acknowledgements

We thank Z.Donalek and J.-L. Lemaire for providing data. We are grateful for partial financial support from NSF, Astronomy & Astrophysics Division (Grants No. 0908108 and No. 1311958) and NASA (Grant No. NNX12AF38G).

References

1 D. A. Williams, *J. Phys: Conference Series*, 2005, **6**, 1–17.
2 R. T. Garrod, S. L. W. Weaver and E. Herbst, *Astrophys. J.*, 2008, **682**, 283–302.
3 G. Vidali, *J. Low Temp. Phys.*, 2013, **170**, 1–30.
4 N. Katz, I. Furman, O. Biham, V. Pirronello and G. Vidali, *Astrophys. J.*, 1999, **522**, 305.
5 V. Pirronello, O. Biham, C. Liu, L. O. Shen and G. Vidali, *Astrophys. J. Lett.*, 1997, **483**, L131.
6 V. Pirronello, C. Liu, L. Shen and G. Vidali, *Astrophys. J.*, 1997, **475**, L69–L72.
7 S. Cazaux and A. G. G. M. Tielens, *Astrophys. J.*, 2004, **604**, 222–237.
8 W. Iqbal, K. Acharyya and E. Herbst, *Astrophys. J.*, 2012, **751**, 58.
9 L. Amiaud, J. H. Fillion, S. Baouche, F. Dulieu, A. Momeni and J. L. Lemaire, *J. Chem. Phys.*, 2006, **124**, 94702.

10 L. Amiaud, F. Dulieu, J.-H. Fillion, a. Momeni and J. L. Lemaire, *J. Chem. Phys.*, 2007, **127**, 144709.
11 J. A. Noble, E. Congiu, F. Dulieu and H. J. Fraser, *Mon. Not. R. Astron. Soc.*, 2012, **421**, 768–779.
12 J. He, P. Frank and G. Vidali, *Phys. Chem. Chem. Phys.*, 2011, **13**, 15803–9.
13 D. J. Burke and W. a. Brown, *Phys. Chem. Chem. Phys.*, 2010, **12**, 5947–69.
14 S. Sundaresan and K. Kaza, *Surf. Sci.*, 1985, **160**, 103–121.
15 N. Watanabe and A. Kouchi, *Astrophys. J.*, 2002, **571**, L173–L176.
16 H. Hidaka, N. Watanabe, T. Shiraki, A. Nagaoka and A. Kouchi, *Astrophys. J.*, 2004, **614**, 1124–1131.
17 N. Watanabe and A. Kouchi, *Progr. Surf. Sci.*, 2008, **83**, 439–489.
18 G. W. Fuchs, H. M. Cuppen, S. Ioppolo, C. Romanzin, S. E. Bisschop, S. Andersson, E. F. van Dishoeck and H. Linnartz, *Astron. & Astrophys.*, 2009, **505**, 629–639.
19 H. Hidaka, M. Watanabe, A. Kouchi and N. Watanabe, *Phys. Chem. Chem. Phys.*, 2011, **13**, 15798–802.
20 S. Ioppolo, H. M. Cuppen, C. Romanzin, E. F. van Dishoeck and H. Linnartz, *Astrophys. J.*, 2008, **686**, 1474–1479.
21 N. Miyauchi, H. Hidaka, T. Chigai, A. Nagaoka, N. Watanabe and a. Kouchi, *Chem. Phys. Lett.*, 2008, **456**, 27–30.
22 Y. Oba, N. Miyauchi, H. Hidaka, T. Chigai, N. Watanabe and a. Kouchi, *Astrophys. J.*, 2009, **701**, 464–470.
23 F. Dulieu, L. Amiaud, E. Congiu, J.-H. Fillion, E. Matar, A. Momeni, V. Pirronello and J. L. Lemaire, *Astron. & Astrophys.*, 2010, **512**, A30.
24 D. Jing, J. He, J. Brucato, A. De Sio, L. Tozzetti and G. Vidali, *Astrophys. J.*, 2011, **741**, L9.
25 D. Jing, J. He, J. J. R. Brucato, G. Vidali, L. Tozzetti and A. De Sio, *Astrophys. J.*, 2012, **756**, 98.
26 R. Kaiser, G. Eich, A. Gabrysch and K. Roessler, *Astron. & Astrophys.*, 1999, **346**, 340–344.
27 J. He, K. Gao and G. Vidali, *Astrophys. J.*, 2010, **721**, 1656–1662.
28 F. Mispelaer, P. Theulé, H. Aouididi, J. Noble, F. Duvernay, G. Danger, P. Roubin, O. Morata, T. Hasegawa and T. Chiavassa, *Astron. & Astrophys.*, 2013, **555**, A13.
29 J. He, D. Jing and G. Vidali, *Phys. Chem. Chem. Phys.*, 2013, submitted.
30 T. Zubkov, R. S. Smith, T. R. Engstrom and B. D. Kay, *J. Chem. Phys.*, 2007, **127**, 184707.
31 J. E. Roser, G. Vidali, G. Manicò and V. Pirronello, *Astrophys. J.*, 2001, **555**, L61–L64.
32 G. Antczak and G. Ehrlich, *Surf. Sci.*, 2005, **589**, 52–66.
33 H. B. Perets, O. Biham, G. Manico, V. Pirronello, J. Roser, S. Swords and G. Vidali, *Astrophys. J.*, 2005, **627**, 850–860.
34 H. B. Perets, A. Lederhendler, O. Biham, G. Vidali, L. Li, S. Swords, E. Congiu, J. Roser, G. Manicó, J. R. Brucato and V. Pirronello, *Astrophys. J.*, 2007, **661**, L163–L166.
35 T. Stantcheva, V. I. Shematovich and E. Herbst, *Astron. & Astrophys.*, 2002, **391**, 1069–1080.
36 J. Le Bourlot, F. Le Petit, C. Pinto, E. Roueff and F. Roy, *Astron. & Astrophys.*, 2012, **541**, A76.
37 Y. Oba, N. Watanabe, T. Hama, K. Kuwahata, H. Hidaka and A. Kouchi, *Astrophys. J.*, 2012, **749**, 67.
38 T. Hama, K. Kuwahata, N. Watanabe, A. Kouchi, Y. Kimura, T. Chigai and V. Pirronello, *Astrophys. J.*, 2012, **757**, 185.
39 V. Pirronello, C. Liu, J. E. Roser and G. Vidali, *Astron. & Astrophys.*, 1999, **344**, 681–686.
40 Z. Dohnálek, G. a. Kimmel, S. a. Joyce, P. Ayotte, R. S. Smith and B. D. Kay, *J. Phys. Chem. B*, 2001, **105**, 3747–3751.
41 J. T. Yates, *Methods of Experimental Physics: Solid State Physics: Surfaces*, Academic Press, 1985, vol. 22, p. 425.
42 K. W. Kolasinki, *Surface science : foundations of catalysis and nanoscience*, Wiley: Hoboken, N.J., 2008.
43 M. P. Collings, M. A. Anderson, R. Chen, J. W. Dever, S. Viti, D. A. Williams and M. R. S. McCoustra, *Mon. Not. R. Astron. Soc.*, 2004, **354**, 1133–1140.
44 S. E. Bisschop, H. J. Fraser, K. I. Öberg, E. F. van Dishoeck and S. Schlemmer, *Astron. & Astrophys.*, 2006, **449**, 1297–1309.
45 L. Hornekaer, a. Baurichter, V. V. Petrunin, a. C. Luntz, B. D. Kay and a. Al-Halabi, *J. Chem. Phys.*, 2005, **122**, 124701.
46 G. Vidali and L. Li, *J. Phys. Conden. Mat.*, 2010, **22**, 304012.
47 P. J. Barrie, *Phys. Chem. Chem. Phys.*, 2008, **10**, 1688–96.

48 Y. Tovbin, *Progr. Surf. Sci.*, 1990, **34**, 1–235.
49 B. Meng and W. Weinberg, *Surf. Sci.*, 1997, **374**, 443–453.
50 A. Šurda and I. Karasova, *Surf. Sci.*, 1981, **109**, 605–620.
51 Yldz, Umut A., Acharyya, Kinsuk, Goldsmith, Paul F., van Dishoeck, Ewine F., Melnick, Gary, Snell, Ronald, Liseau, Ren, Chen, Jo-Hsin, Pagani, Laurent, Bergin, Edwin, Caselli, Paola, Herbst, Eric, Kristensen, Lars E., Visser, Ruud, Lis, Dariusz C. and Gerin, Maryvonne, *Astron. & Astrophys.*, 2013, **558**, A58.
52 L. Bruch, R. Diehl and J. Venables, *Rev. Mod. Phys.*, 2007, **79**, 1381–1454.
53 G. Vidali, L. Li, H. Zhao, Y. Frank, I. Lohmar, H. B. Perets and O. Biham, *J. Phys. Chem. A*, 2010, **114**, 10575–83.
54 S. Nordholm, *Chem. Phys.*, 1985, **98**, 367–379.
55 E. Herbst and H. M. Cuppen, *Proc. Natl. Academy Sci.*, 2006, **103**, 12257–62.